JOURNAL OF SOLID STATE CHEMISTRY 114, 66–72 (1995)

Preparation, Structure Refinement, and Properties of Some Compounds with $Dy_2Fe_2Si_2C$- and $LaMn_{11}C_{2-x}$-Type Structure

R. Pöttgen, T. Ebel, C. B. H. Evers, and W. Jeitschko

Anorganisch-Chemisches Institut, Universität Münster, Wilhelm-Klemm-Strasse 8, D-48149 Münster, Germany

Received November 18, 1993; in revised form March 22, 1994; accepted March 24, 1994

The new compounds $Tm_2Fe_2Si_2C$ and $Lu_2Fe_2Si_2C$ were prepared by arc-melting cold-pressed pellets of the elemental components. They crystallize with the monoclinic $Dy_2Fe_2Si_2C$-type structure. The crystal structure of $Tm_2Fe_2Si_2C$ was refined from single-crystal X-ray data: $C2/m$, $a = 1049.7(3)$ pm, $b = 388.2(1)$ pm, $c = 664.6(2)$ pm, $\beta = 128.96(2)°$, $R = 0.020$ for 296 structure factors, and 21 variable parameters. The structure may be considered as consisting of two-dimensionally infinite polyanionic layers of $[Fe_2Si_2C^{6-}]_n$ separated by the rare-earth cations. The hydrolysis of $Er_2Fe_2Si_2C$ with diluted hydrochloric acid yields mainly methane besides about 20 wt% of C_2 and C_3 hydrocarbons. $Tm_2Fe_2Si_2C$ orders antiferromagnetically at $T_N = 2.7(2)$ K. The magnetization behavior for this compound suggests metamagnetism. $Lu_2Fe_2Si_2C$ is Pauli paramagnetic. Electrical conductivity measurements of polycrystalline samples of $Tm_2Fe_2Si_2C$ and $Lu_2Fe_2Si_2C$ indicate metallic conductivity. $ThFe_{10}SiC_{2-x}$ has a tetragonal $LaMn_{11}C_{2-x}$-type structure with the lattice constants $a = 1005.3(2)$ pm and $c = 651.6(2)$ pm.

INTRODUCTION

The first structurally well-characterized ternary silicide carbide was the Nowotny-phase Mo_5Si_3C (1). Ti_3SiC_2 was reported only two years later (2). More recently the series of ternary compounds $Ln_5Si_3C_x$ with filled Cr_5B_3- and Mn_5Si_3-type structure has been investigated (3–7). In all these silicide carbides the carbon atoms occupy octahedral voids formed by the metal atoms. Recently the ternary silicide carbides $U_3Si_2C_2$ and $U_{20}Si_{16}C_3$ were reported (8). The carbon atoms in $U_{20}Si_{16}C_3$ occupy octahedral voids formed by six uranium atoms, while the carbon and silicon atoms in $U_3Si_2C_2$ form Si–C units, which are surrounded by nine uranium atoms. The quaternary systems of the rare-earth elements with iron, silicon, and carbon were investigated recently by Paccard, Paccard, Bertrand, and co-workers (9–11) while searching for new permanent magnets. These investigations resulted in the new compounds $DyFe_2SiC$ (9), $R_2Fe_2Si_2C$ (R = Y, Pr, Nd, and Gd–Er) with $Dy_2Fe_2Si_2C$-type structure (10), and $RFe_{10}SiC_{0.5}$ (R = Ce–Nd, Sm) (11) with $LaMn_{11}C_{2-x}$-type structure (12). The magnetic properties of the compounds $R_2Fe_2Si_2C$ with R = Y, Pr, Nd and Gd–Er were also investigated (13, 14). The isotypic series AFe_2SiC (A = Y, Sm, Gd, Tb, Ho, Er, Tm, Lu, Th, and U) with $DyFe_2SiC$-type structure was published recently (15). In the present paper we report mainly about the structural and physical properties of the silicide carbides $Tm_2Fe_2Si_2C$ and $Lu_2Fe_2Si_2C$.

SAMPLE PREPARATION

Starting materials were filings of the rare-earth metals (>99.9%), thorium ingots (nominal purity 99.9%), iron powder (Alpha, 99.9%, 325 mesh), silicon powder (Fluka, >99.9%, 100 mesh), and graphite flakes (Alpha, >99.5%, 20 mesh). Filings of thorium were prepared under dried paraffin oil. They were washed with dried cyclohexane under argon. The thorium filings were not allowed to contact air prior to the reactions. The samples were prepared by arc-melting of small (about 500 mg) cold-pressed pellets of the elemental components of the ideal compositions in an argon (99.996%) atmosphere. The argon was further purified by repeatedly melting a titanium button prior to the reactions. The samples were wrapped in tantalum foil and annealed in evacuated silica tubes for 30 days at 1000°C. Single crystals of $Tm_2Fe_2Si_2C$ were obtained by annealing an arc-melted button in an evacuated, water-cooled silica tube in a high-frequency furnace slightly below the melting point for about 4 hr.

CHEMICAL PROPERTIES

The quaternary silicide carbides are all stable in air for several months. Single crystals of these compounds are grey with metallic luster. Powdered samples are dark grey. While the samples do not visibly react with water, the hydrolysis with diluted hydrochloric acid proceeds rather fast. A sample of $Er_2Fe_2Si_2C$ was hydrolyzed with $2N$ hydrochloric acid at room temperature. The emerging gaseous products (H_2 and hydrocarbons) were analyzed in a mass spectrometer (CH5, Varian MAT, 20°C, 70 eV). Of the hydrocarbons about 80 ± 5 wt% was methane

0022-4596/95 $6.00

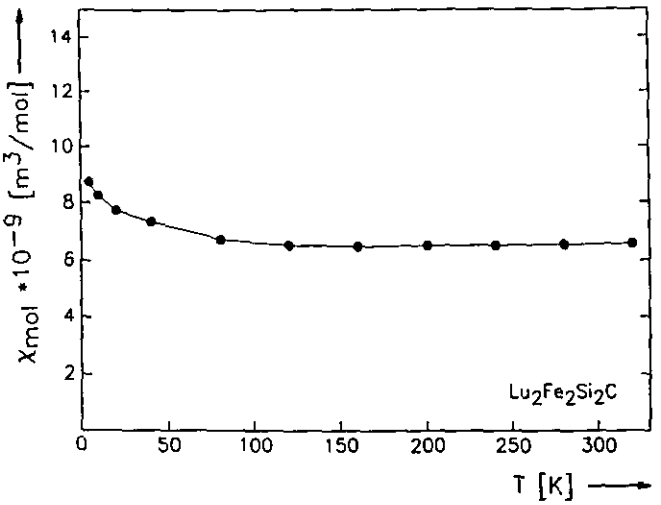

FIG. 1. The magnetic susceptibility of $Lu_2Fe_2Si_2C$ as a function of temperature.

besides about 20 ± 5 wt% of C_2 and C_3 hydrocarbons. Nevertheless, the compound contains only isolated carbon atoms. The occurrence of the C_2 and C_3 hydrocarbons is probably due to catalytic effects of the iron atoms. Similar mixtures of hydrolyses products were observed for various ternary carbides containing transition metals (16), while CaC_2 and Al_4C_3 are known to yield only C_2H_2 and CH_4, respectively. Energy dispersive analysis of the quaternary silicide carbides in a scanning electron microscope were in agreement with the ideal compositions and did not reveal any impurity elements heavier than sodium.

MAGNETIC SUSCEPTIBILITIES OF $Tm_2Fe_2Si_2C$ AND $Lu_2Fe_2Si_2C$

Susceptibility measurements of the two carbides were carried out in the temperature range between 2 and 300 K with a SQUID magnetometer (S. H. E. Quantum Design, Inc.) with magnetic flux densities of up to 5.5 T as described previously (17, 18). The susceptibilities of $Lu_2Fe_2Si_2C$ were very small, not field-dependent, with a room temperature value of $6.6\ (\pm 0.1) \cdot 10^{-9}$ m^3/mol, and almost temperature-independent, suggesting Pauli paramagnetism (Fig. 1). The small upturn at low temperatures is most likely due to a very minor amount of a paramagnetic impurity. For an approximate diamagnetic correction we assumed the atomic susceptibilities (in units of 10^{-9} m^3/mol) of −0.21 (Lu^{3+}), −0.16 (Fe^{2+}), and −0.02 (Si^{4+}) given by Klemm (19), and −0.001 (C) given by Haberditzel (20). With the thus calculated correction of $\chi_{dia} = -0.8 \cdot 10^{-9}$ m^3/mol a value of $\chi = 7.4\ (\pm 0.1) \cdot 10^{-9}$ m^3/mol is obtained for the Pauli paramagnetism of the conduction electrons. Thus, there is no magnetic contribution from the iron atoms.

The susceptibility behavior of $Tm_2Fe_2Si_2C$ is dominated by the Tm^{3+} ions. At temperatures above 20 K $Tm_2Fe_2Si_2C$ shows Curie–Weiss behavior with a slight field dependence, most likely due to an unknown ferromagnetic impurity, although the Guinier powder diagram gave no indication for such an impurity. The susceptibilities obtained with magnetic flux densities of 3 and 5 T were practically the same and thus the impurity content was very small. The compound orders antiferromagnetically at low temperatures with a Néel temperature of $T_N = 2.7 \pm 0.2$ K (Fig. 2). The magnetic moment $\mu_{exp} = 7.8 \pm 0.1\ \mu_B$, calculated from the slope of the $1/\chi$ vs T plot according to $\mu_{exp} = 2.83[(\chi/2)(T - \Theta)]^{1/2}\ \mu_B$ agrees rather well with the free ion value of $\mu_{eff} = 7.56\ \mu_B$ calculated from the formula $\mu_{eff} = g[J(J+1)]^{1/2}\ \mu_B$. The Weiss constant of $\Theta = 14 \pm 1$ K was determined by linear extrapolation of the high-temperature part of the $1/\chi$ vs T plot to $1/\chi = 0$.

At low temperatures the magnetic susceptibility of $Tm_2Fe_2Si_2C$ became field-dependent in a way suggesting metamagnetism. The value of the critical field strength was estimated to be 0.4 T (Inset of Fig. 2). This was confirmed by the magnetization measurements at 2 K (Fig. 3), which nearly show magnetic saturation at the highest obtainable field of 5.5 T. The hysteresis loop expected for a metamagnet was too small to be observable in the 2 K data, because this temperature is too close to the ordering temperature of $T_N = 2.7$ K. The magnetic moment per Tm atom, calculated from the highest obtainable magnetization of 5.5 T (nearly the saturation magnetisation, sm), amounts $\mu_{exp(sm)} = 4.5 \pm 0.1\ \mu_B$. This

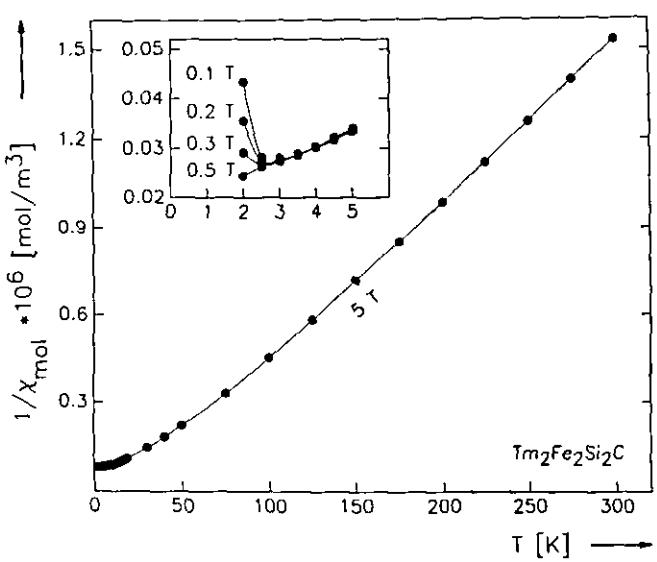

FIG. 2. The temperature dependence of the reciprocal susceptibility of $Tm_2Fe_2Si_2C$ measured with a magnetic flux density of 5 Tesla. The inset shows the low-temperature behavior of the reciprocal susceptibility with smaller flux densities.

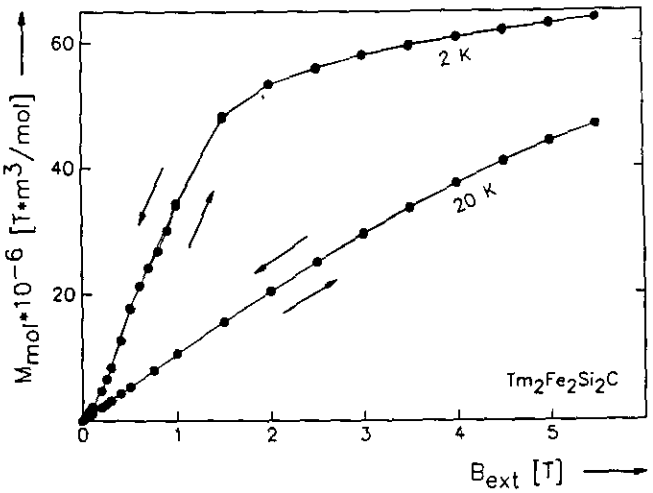

FIG. 3. Magnetization M_{mol} vs magnetic flux density B_{ext} of $Tm_2Fe_2Si_2C$ at 2 and 20 K.

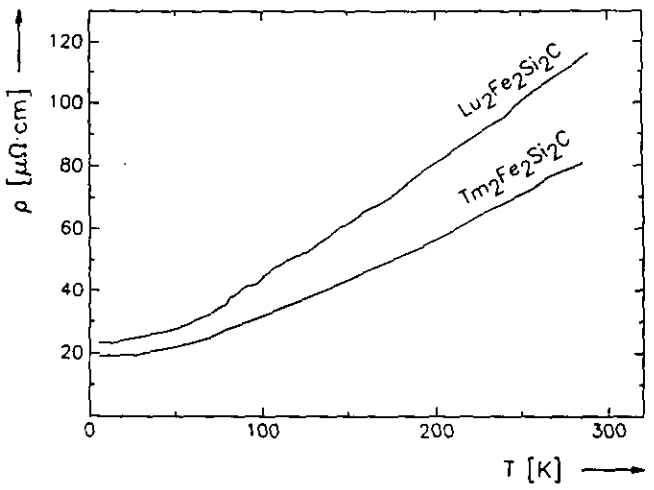

FIG. 5. Electrical resistivity of $Tm_2Fe_2Si_2C$ and $Lu_2Fe_2Si_2C$ as a function of temperature.

may be compared to the theoretical saturation moment of $\mu_{calc(sm)} = 7.0\ \mu_B$, calculated according to $\mu_{calc(sm)} = g * J\ \mu_B$, where g is the Landé factor and J is the total angular momentum quantum number. Thus, the experimental value is somewhat smaller than the theoretical value, as expected for a powder sample with random orientation of the particles.

The Néel temperatures of $Tm_2Fe_2Si_2C$ and the corresponding silicide carbides $R_2Fe_2Si_2C$ (R = Nd, Gd, Tb, Dy, and Er) (13) seem to follow the de Gennes function (21), which states that the Néel temperatures are proportional to $(g - 1)^2J(J + 1)$ (Fig. 4). Only the gadolinium compound shows a strong deviation from this function. The validity of the calculated de Gennes transition temperatures, however, is restricted to comparable structures (22) and the magnetization measurements of $Gd_2Fe_2Si_2C$ (13) had shown that the magnetic behavior of this compound is completely different from that of the others.

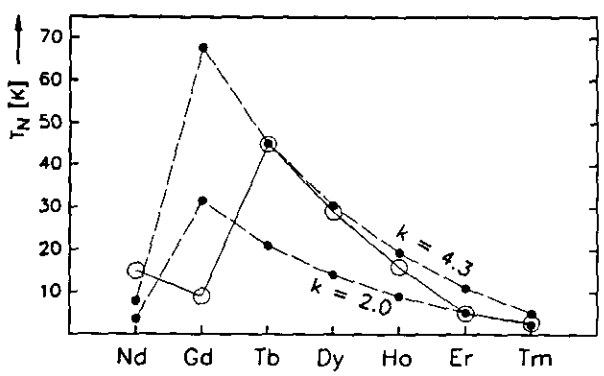

FIG. 4. Néel temperatures of $Dy_2Fe_2Si_2C$-type compounds. The de Gennes functions $T_N \approx k(g - 1)^2J(J + 1)$ for the arbitrarily chosen values of k = 4.3 and k = 2 are drawn with dashed lines.

The magnetic structures of the isotypic neodymium and terbium compounds have been reported recently (14). According to these investigations the iron atoms carry small magnetic moments of 1.5 μ_B and 1.3 μ_B, respectively, while we have not observed any magnetic moments for the iron atoms in the isotypic thulium and lutetium compounds. We therefore thought about the possibility that the magnetic moments of the iron atoms of these compounds might be hidden in an antiferromagnetic structure with a Néel temperature higher than room temperature. However, in agreement with the interpretation of our susceptibility measurements given above, the ^{57}Fe Mössbauer spectra of $Tm_2Fe_2Si_2C$ recorded at 4.2 K and 300 K gave no indication for magnetic order. Both spectra were practically identical and showed no hyperfine field splitting (23).

ELECTRICAL PROPERTIES

The electrical conductivity behavior of $Tm_2Fe_2Si_2C$ and $Lu_2Fe_2Si_2C$ was investigated with an a. c. four-probe device between 4 K and room temperature as described previously (24). Several compact polycristalline samples, all taken from the same arc-melted and annealed ingots, were measured. The samples had typical sizes of about 0.5 × 0.5 × 0.5 mm³ and the results were completely reproducible within a factor of two from sample to sample, while the relative values for one sample at different temperatures are much more reliable. The specific resistivities of both compounds decrease with decreasing temperature (Fig. 5), as is typical for metallic conductors. The absolute values of the resistivities at room temperature are about 100 μΩcm, as compared to the values of ρ = 1.6 μΩcm and ρ = 10 μΩcm found for the metals silver and iron, respectively (25).

LATTICE CONSTANTS

The powdered samples were characterized by the Guinier technique with $CuK\alpha_1$ radiation using α-quartz (a = 491.30 pm, c = 540.46 pm) as an internal standard. Indices could be assigned on the basis of the C-centered monoclinic cell as found previously for $Dy_2Fe_2Si_2C$ (10). The following lattice constants were obtained by least-squares fits. The standard deviations in the place value of the last listed digit are given in parentheses (throughout the paper); $Tm_2Fe_2Si_2C$: a = 1049.7(3) pm, b = 388.2(1) pm, c = 664.2(2) pm, β = 128.96(2)°, V = 0.2105 nm^3; $Lu_2Fe_2Si_2C$: a = 1045.1(2) pm, b = 386.1(1) pm, c = 660.0(1) pm, β = 128.88(2)°, and V = 0.2073 nm^3.

While searching for an isotypic compound with thorium as the most electropositive component we obtained the new compound $ThFe_{10}SiC_{2-x}$. This compound has the tetragonal lattice constants a = 1005.3(2) pm, c = 651.6(2) pm, and V = 0.6585 nm^3. A powder pattern calculated (26) with the positional parameters of $NdFe_{10}SiC_{0.5}$ (11) gave good agreement between the observed and calculated intensities and thus this compound is isotypic with the corresponding lanthanoid compounds $RFe_{10}SiC_{0.5}$ (R = Ce, Pr, Nd, Sm) (11) and $LaMn_{11}C_{2-x}$ (12).

CRYSTAL STRUCTURE OF $Tm_2Fe_2Si_2C$

Single crystals of $Tm_2Fe_2Si_2C$ were isolated from the crushed sample prepared in the high-frequency furnace. They were investigated with a Buerger precession camera to establish their symmetry and suitability for intensity data collection. The precession photographs showed monoclinic symmetry and the systematic extinctions for a C-centered lattice. The structure was eventually refined in the centrosymmetric space group $C2/m$ (No. 12).

Single-crystal intensity data were collected on an automated four-circle diffractometer with graphite monochromated Mo$K\alpha$ radiation and a scintillation counter with pulse-height discrimination. The crystallographic data and some results are summarized in Table 1. The structure of $Tm_2Fe_2Si_2C$ was assumed to be isotypic with $Dy_2Fe_2Si_2C$ (10), which was confirmed during the full-matrix least-squares refinements with atomic scattering factors (27), corrected for anomalous dispersion (28). A factor accounting for isotropic secondary extinction was also refined and applied to the calculated structure factors. The weighting scheme included a term accounting for the counting statistics. To check for deviations from the ideal composition the scale factor was held constant in one series of least-squares cycles and all occupancy parameters were allowed to vary along with the thermal parameters. No significant deviations from the full occupancies were found, and in the final least-squares cycles the ideal occupancies were assumed. The metal and silicon atoms were refined with anisotropic and the carbon atoms with isotropic thermal parameters. The final conventional and weighted residuals are R = 0.020 and R_w = 0.029 for 296 structure factors and 21 variable parameters. A final difference Fourier analysis showed the value of 0.89 e/Å^3 as highest residual density, too small and too close to a metal site to be suitable for an additional atomic position. The atomic parameters and the interatomic distances are listed in Tables 2 and 3. A projection of the structure and the coordination polyhedra is shown in Fig. 6. Listings of the structure factor tables and the anisotropic thermal parameters are available from the authors.

The present structure refinement of $Tm_2Fe_2Si_2C$ fully

TABLE 1
Crystallographic Data for $Tm_2Fe_2Si_2C$

Lattice constants	a = 1049.7(3) pm b = 388.2(1) pm c = 664.2(2) pm β = 128.96(2)° V = 0.2105 nm^3
Formula units/cell	Z = 2
Space group	$C2/m$ (No. 12)
Formula weight	517.7
Calculated density (g/cm^3)	ρ_c = 8.17
Absorption coefficient (cm^{-1})	μ(Mo$K\alpha$) = 493
Crystal dimensions (μm^3)	20 × 20 × 110
$\theta/2\theta$ scans up to	2θ = 60°
Range in hkl	±14, ±5, ±9
Total number of reflections	1595
Absorption correction	from psi scans
Transmission coefficient (highest/lowest)	1.23
Unique reflections	350
Inner residual	R_i = 0.024
Reflections with $I > 3\sigma(I)$	296
Number of variables	21
Extinction correction value, g^a	1.15(8) × 10^{-6}
Conventional residual (on F values)	R = 0.020
Weighted residual	R_w = 0.029

[a] The extinction correction value g is defined by corr. factor $1/(1 + g \times I_c)$.

TABLE 2
Atomic Parameters of $Tm_2Fe_2Si_2C$[a]

Atom	$C2/m$	Occupancy	x	y	z	B
Tm	4i	1.000(2)	0.56098(5)	0	0.29255(8)	0.396(8)
Fe	4i	1.001(5)	0.2042(2)	0	0.0996(3)	0.41(3)
Si	4i	0.97(1)	0.1534(3)	0	0.7026(5)	0.52(6)
C	2a	0.93(5)	0	0	0	0.6(3)

[a] The last column contains the isotropic thermal parameter of the carbon atom and the equivalent isotropic thermal parameters B (× 100, in units of nm^2) of the metal atoms. The occupancy parameters were refined in separate least-squares cycles. In the final cycles the ideal occupancies were assumed.

TABLE 3
Interatomic Distances (pm) in the Structure of $Tm_2Fe_2Si_2C$[a]

Tm:	2 C	252.8	Fe:	1 C	180.2
	2 Si	296.8		2 Si	229.3
	1 Si	297.8		1 Si	234.0
	2 Si	298.8		2 Fe	283.6
	2 Fe	303.1		2 Tm	303.1
	1 Fe	310.3		1 Tm	310.3
	1 Fe	314.2		1 Tm	314.2
	2 Fe	317.8		2 Tm	317.8
	1 Tm	324.0			
	1 Si	354.7	Si:	2 Fe	229.3
	2 Tm	365.5		1 Fe	234.0
	1 Tm	369.9		1 Si	259.2
	2 Tm	388.2		2 Tm	296.8
				1 Tm	297.8
				2 Tm	298.8
				1 Tm	354.7
			C:	2 Fe	180.2
				4 Tm	252.8

[a] All distances shorter than 480 pm (Tm–Tm, Tm–Si), 400 pm (Tm–Fe, Tm–C, Fe–Si, Fe–C), 360 pm (Fe–Fe, Si–Si, C–C), and 320 pm (Si–C) are listed. Standard deviations are all equal to or less than 0.3 pm.

confirms the earlier structure determination of $Dy_2Fe_2Si_2C$ (10). In several rare-earth transition metal carbides the carbon positions were found with considerable deviations from the full occupancy, interestingly, so far only for carbides with very high metal content. For example, in the carbides $CeRhC_2$ (29), $Gd_3Mn_2C_6$ (30) and Er_2FeC_4 (31) the carbon positions were found to be fully occupied, while the occupancy of at least some carbon positions is only between 59 and 81% in $LaMn_{11}C_{2-x}$ (12), $Pr_2Mn_{17}C_{3-x}$ (32), $Tb_2Mn_{17}C_{3-x}$ (33), and $Ce_2Ni_{22}C_{3-x}$ (24).

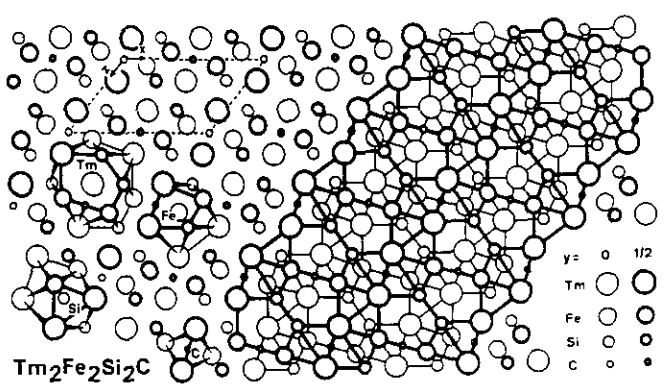

FIG. 6. Crystal structure and coordination polyhedra of $Tm_2Fe_2Si_2C$. Atoms connected by thick and thin lines in the right-hand part of the drawing are at $y = \frac{1}{2}$ and $y = 0$, respectively.

In $Tm_2Fe_2Si_2C$ the carbon position is essentially fully occupied, as was found also for $U_3Si_2C_2$ and $U_{20}Si_{16}C_3$ (8).

The carbon atoms in the $Dy_2Fe_2Si_2C$-type structure have octahedral metal coordination as in most frequently observed for "isolated" carbon atoms (carbon atoms without C–C bonds). In the $Dy_2Fe_2Si_2C$-type carbides the carbon atoms have four rare-earth atoms as neighbors forming a square with two iron atoms in *trans*-position completing the flattened octahedron. Analogous environments were found for the carbon atoms in $UMoC_2$ (34), YCoC (35), $U_5Re_3C_8$ (36), Pr_2ReC_2 (37), and $Sc_5Re_2C_7$ (38).

The interaction of the rare-earth atoms with the neighboring atoms may be considered as primarily ionic, resulting in a formula $[2Tm^{3+}]^{6+}[Fe_2Si_2C]^{6-}$. Together, the iron, silicon, and carbon atoms form a polyanion. The Si–Si bonds of 259 pm are rather long in view of the Si–Si bond distance of 235 pm in elemental silicon (39). If, for simplicity, this very weak bond is neglected, the polyanion may be regarded as essentially two-dimensionally infinite (Fig. 7). We believe that the atomic arrangement and chemical bonding of highly condensed solid-state compounds are governed by rules similar to those found for molecular compounds. Thus, all valence orbitals should possibly be utilized for chemical bonding, i.e., the iron atoms might be expected to follow the 18-electron rule and the silicon and carbon atoms should obey the octet rule. In aiming for such a visualization of the chemical bonding, we have used the classical Lewis formalism to see how these rules are fulfilled for $Tm_2Fe_2Si_2C$. In the lower part of Fig. 7 the polyanion is shown together with two different valence electron distributions. The five-membered Si–Fe–C–Fe–Si zigzag chains of the monomer are connected like the bricks in a wall. Each brick of the monomer $[Fe_2Si_2C]^{6-}$ has to contain 34 valence electrons: 16 from the two iron atoms, 8 from the two silicon atoms, 4 from the carbon atom, and 6 from the formal charge. The iron–carbon interactions are shown as double bonds and the iron–silicon interactions as single bonds. The remaining electrons are shown as lone pairs at the silicon atoms and as nonbonding electrons (dots) at the iron atoms. In the visualization at the left side of Fig. 7 the iron atoms obtain a total of 15 valence electrons including 5 nonbonding electrons. Using two of the latter (at the right side of Fig. 7) to form Fe–Fe bonds, each iron atom attains 17 electrons. This is as close as one can get to the 18-electron rule without invoking fractional bonds. The assumption that there is some Fe–Fe bonding is supported not only by the length of the Fe–Fe distance of 284 pm, but, more conclusive, also from the small Fe–Si–Fe bond angle of 75°. The Fe–C distance of 180 pm is slightly shorter than the Fe–C distances of 181 and 183 pm in $Fe(CO)_5$, and there is generally agreement that the Fe–C distances of the carbonyls have some double bond character (40). Thus, there is at least some justification for the

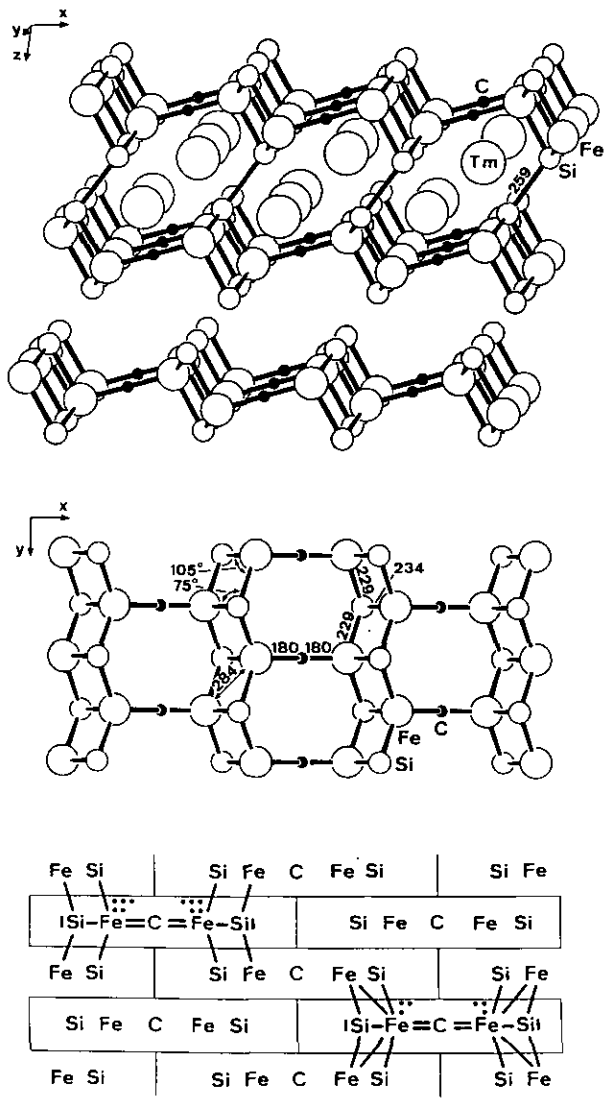

FIG. 7. The polyanionic iron–silicon–carbon network in the structure of $Tm_2Fe_2Si_2C$. In the upper part of the figure the whole structure is shown in a view projected approximately along the y direction. In the lower part of that projection the Tm atoms are omitted for clarity and the relatively weak Si–Si bonds of 259.2 pm are left out, thus emphasizing the two-dimensionally infinite character of the polyanion. A view of the polyanion perpendicular to the xy plane is shown in the middle of the figure with some bond angles and distances (pm). At the bottom the same atoms are shown with two different valence electron distributions using the Lewis formalism. On the left side the iron atoms obtain 15 valence electrons and on the right side they obtain 17. However, this should not imply that they carry magnetic moments, as discussed in the text.

simple representation of chemical bonding as shown in Fig. 7. Nevertheless, such a picture must have shortcomings. The Pauli paramagnetism of $Lu_2Fe_2Si_2C$ indicates that there are no localized moments at the iron atoms and the metallic conductivity shows that the electrons at the Fermi level are delocalized in an unfilled band. Certainly, a band structure description is better suited to represent the chemical bonding, especially for the electrons at the Fermi level of this extended solid.

ACKNOWLEDGMENTS

This work was supported by the Deutsche Forschungsgemeinschaft. We also thank Dr. M. H. Möller and Dipl.-Ing. U. Rodewald for the collection of the diffractometer data, Mr. K. Wagner for the work at the scanning electron microscope, Mr. H. Rabeneck for the analyses of the hydrolyses products, and Mrs. U. Göcke for the help with the drawings. We are grateful to Dr. G. Höfer (Heraeus Quarzschmelze) for a generous gift of silica tubes. And last but not least we acknowledge the Stiftung Stipendienfonds des Verbandes der Chemischen Industrie for the stipend to R. P.

REFERENCES

1. E. Parthé, W. Jeitschko, and V. Sadagopan, *Acta Crystallogr.* **19,** 1031 (1965).
2. W. Jeitschko and H. Nowotny, *Monatsh. Chem.* **98,** 329 (1967).
3. G. Y. M. Al-Shahery, D. W. Jones, I. J. McColm, and R. Steadman, *J. Less-Common Met.* **85,** 233 (1982).
4. G. Y. M. Al-Shahery, D. W. Jones, I. J. McColm, and R. Steadman, *J. Less-Common Met.* **87,** 99 (1982).
5. G. Y. M. Al-Shahery, R. Steadman, and I. J. McColm, *J. Less-Common Met.* **92,** 329 (1983).
6. T. W. Button and I. J. McColm, *J. Less-Common Met.* **97,** 237 (1984).
7. G. Y. M. Al-Shahery and I. J. McColm, *J. Less-Common Met.* **98,** L5 (1984).
8. R. Pöttgen, D. Kaczorowski, and W. Jeitschko, *J. Mater. Chem.* **3,** 253 (1993).
9. L. Paccard, D. Paccard, and C. Bertrand, *J. Less-Common Met.* **135,** L5 (1987).
10. L. Paccard and D. Paccard, *J. Less-Common Met.* **136,** 297 (1988).
11. J. Le Roy, J. M. Moreau, C. Bertrand, and M. A. Fremy, *J. Less-Common Met.* **135,** 19 (1987).
12. W. Jeitschko and G. Block, *Z. Anorg. Allg. Chem.* **528,** 61 (1985).
13. D. Schmitt, D. Paccard, and L. Paccard, *Solid State Commun.* **84,** 357 (1992).
14. J. Le Roy, D. Paccard, C. Bertrand, J. L. Soubeyroux, J. Bouillot, L. Paccard, and D. Schmitt, *Solid State Commun.* **86,** 675 (1993).
15. A. M. Witte and W. Jeitschko, *J. Solid State Chem.* **112,** 232 (1994).
16. W. Jeitschko, M. H. Gerss, R.-D. Hoffmann, and S. Lee, *J. Less-Common Met.* **56,** 397 (1989).
17. M. Reehuis, T. Vomhof, and W. Jeitschko, *J. Less-Common Met.* **169,** 139 (1991).
18. K. Zeppenfeld, R. Pöttgen, M. Reehuis, W. Jeitschko, and R. K. Behrens, *J. Phys. Chem. Solids* **54,** 257 (1993).
19. W. Klemm, *Z. Anorg. Allg. Chem.* **246,** 347 (1941).
20. W. Haberditzel, *Magnetochemie*, Akademie-Verlag, Berlin (1968).
21. P. G. De Gennes, *C.R. Acad. Sci. Paris* **247,** 1836 (1958).
22. A. Szytuła, *in* "Handbook of Magnetic Materials" (K. H. J. Buschow, Ed.), Vol. 6, pp. 85–180. Elsevier, Amsterdam (1991).
23. M. Prill, B. D. Mosel, and W. Müller-Warmuth, private communication, 1993.
24. R. Pöttgen, W. Jeitschko, C. Evers, and M. A. Moss, *J. Alloys Compd.* **186,** 223 (1992).
25. R. C. Weast (Ed.), Handbook of Chemistry and Physics, 58th ed., CRC Press, Palm Beach, Florida, 1978.
26. K. Yvon, W. Jeitschko, and E. Parthé, *J. Appl. Crystallogr.* **10,** 73 (1977).

27. D. T. Cromer and J. B. Mann, *Acta Crystallogr.* **24,** 321 (1968).
28. D. T. Cromer and D. Liberman, *J. Chem. Phys.* **53,** 1891 (1970).
29. R.-D. Hoffmann, W. Jeitschko, and L. Boonk, *Chem. Mater.* **1,** 580 (1989).
30. G. E. Kahnert and W. Jeitschko, *Z. Anorg. Allg. Chem.* **619,** 93 (1993).
31. M. H. Gerss, W. Jeitschko, L. Boonk, J. Nientiedt, J. Grobe, E. Mörsen, and A. Leson, *J. Solid State Chem.* **70,** 19 (1987).
32. G. Block and W. Jeitschko, *Inorg. Chem.* **25,** 279 (1986).
33. G. Block and W. Jeitschko, *J. Solid State Chem.* **70,** 271 (1987).
34. D. T. Cromer, A. C. Larson, and R. B. Roof, Jr., *Acta Crystallogr.* **17,** 272 (1994).
35. M. H. Gerss and W. Jeitschko, *Z. Naturforsch., B* **41,** 946 (1986).
36. G. Block and W. Jeitschko, *Monatsh. Chem.* **119,** 319 (1988).
37. W. Jeitschko, G. Block, G. E. Kahnert, and R. K. Behrens, *J. Solid State Chem.* **89,** 191 (1990).
38. R. Pöttgen and W. Jeitschko, *Z. Naturforsch., B* **47,** 358 (1992).
39. J. Donohue, "The Structures of the Elements," Wiley, New York 1974.
40. Ch. Elschenbroich and A. Salzer, "Organometallchemie," 3rd ed. Teubner, Stuttgart, 1990.